Nanoscale

ROYAL SOCIETY OF CHEMISTRY

PAPER

View Article Online
View Journal | View Issue

Cite this: *Nanoscale*, 2025, **17**, 1007

Nano onions based on an amphiphilic Au_3(pyrazolate)$_3$ complex†‡

Atena B. Solea, [a] Davide Dermutas,[a] Farzaneh Fadaei-Tirani, [a] Luigi Leanza, [b] Massimo Delle Piane, [b] Giovanni M. Pavan [b,c] and Kay Severin [a]*

Received 23rd September 2024,
Accepted 18th November 2024

DOI: 10.1039/d4nr03901g

rsc.li/nanoscale

Multilayer vesicles with an onion-like architecture can form by self-assembly of organic amphiphiles such as dendrimers, small-molecule surfactants, and block copolymers. Thus far, there are limited reports about multilayer vesicles based on coordination compounds. Herein, we show that nano onions are obtained by aggregation of an amphiphilic Au_3(pyrazolate)$_3$ complex in aqueous solution. The nanostructures were characterized by cryogenic and transition electron microscopy, dynamic light scattering, and energy-dispersive X-ray analysis. Control experiments with analogous Ag(I) and Cu(I) complexes revealed the importance of Au(I) for the formation of well-defined nano onions. A structurally related Au(I) complex without solubilizing polyethylene glycol side chains was analyzed by single-crystal X-ray diffraction. In the solid state, columns of offset, π-stacked Au_3(pyrazolate)$_3$ complexes are observed, but short intermolecular Au···Au contacts were not found. Molecular dynamics simulations provided further insights into the aggregation process in aqueous solution, supporting the formation of nano-onion structures through lateral interactions between stacked complexes.

Introduction

The integration of inorganic coordination compounds into soft matter systems presents an exciting frontier in materials science, offering new avenues for tailoring the mechanical, optical, and functional properties of soft materials.[1] Trinuclear gold(I) complexes with bridging pyrazolate ligands represent interesting building blocks in this context. Initially reported by Bonati in 1974,[2] these compounds display good chemical stability.[3,4] Structural modifications can be readily achieved by variation of the pyrazolate ligand.[4] Moreover, Au_3(pyrazolate)$_3$ complexes are prone to aggregate *via* aurophilic interactions.[4,5] This characteristic provides a unique opportunity to control the assembly of such complexes. It is also worth noting that aggregates of Au_3(pyrazolate)$_3$ complexes are often luminescent.[4]

Several studies have shown that Au_3(pyrazolate)$_3$ complexes can form liquid-crystal phases.[6] Serrano and co-workers have examined pyrazolate ligands with di- and tri-*n*-decyloxyphenyl substituents in position 3 and 5.[6e,f] The resulting Au trimers were found to form columnar mesophases, some of which displayed good stability at room temperature. Concurrent investigations by Kim *et al.* demonstrated that a single long alkyl chain in 4-position of the pyrazolate ligand can be sufficient for the formation of metallomesogens.[6d]

The assembly of Au_3(pyrazolate)$_3$ complexes with functionalized benzyl substituents in 4-position was studied by Aida and co-workers.[6b,7,8] They observed the formation of luminescent organogels[7] or fibers,[8] depending on the nature of the substituents (Fig. 1). Phase transitions of the organogels were found

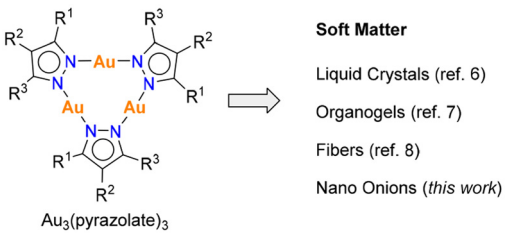

Fig. 1 Au_3(pyrazolate)$_3$ complexes as building blocks for the construction of soft matter.

[a]*Institut des Sciences et Ingénierie Chimiques, École Polytechnique Fédérale de Lausanne (EPFL), 1015 Lausanne, Switzerland. E-mail: kay.severin@epfl.ch*
[b]*Department of Applied Science and Technology, Politecnico di Torino, Torino 10129, Italy*
[c]*Department of Innovative Technologies, University of Applied Sciences and Arts of Southern Switzerland, Lugano, Viganello 6962, Switzerland*

†Computational materials and data pertaining to the study conducted herein (input files, trajectories, *etc.*) are available at: **https://zenodo.org/doi/10.5281/zenodo.13828919**.

‡Electronic supplementary information (ESI) available: Synthetic procedures, experimental and simulation details. CCDC 2357277. For ESI and crystallographic data in CIF or other electronic format see DOI: **https://doi.org/10.1039/d4nr03901g**

to result in pronounced changes in the luminescence properties.

Below, we describe the self-assembly of an amphiphilic Au_3(pyrazolate)$_3$ complex in aqueous solution, leading to the formation of multilayer vesicles with an intriguing onion-like architecture. Self-assembled nano onions have garnered considerable attention in recent years, and numerous experimental[9–15] and computational studies[16] about these systems have appeared. Suited building blocks for the construction of onion-like nanostructures include dendrimers,[9,10] small-molecule surfactants,[11] and block copolymers.[12] Thus far, there are limited reports about multilayer vesicles based on coordination compounds,[13–15] with most efforts focusing on functionalized polyoxometalate complexes.[15] The gold complex reported herein is structurally simple, with only three short polyethylene glycol (PEG) chains attached to a central Au_3(pyrazolate)$_3$ core. Extending the hydrophilic domain by attaching six PEG chains was found to impede nano onion formation. Control experiments with analogous Ag(I) and Cu(I) complexes reveal the importance of Au(I) for generating well-defined vesicles. To complement these experimental observations, we employed molecular dynamics (MD) simulations to gain deeper insight into the self-assembly mechanisms and to explore the role of stacking and lateral interactions in the formation of these unique structures.

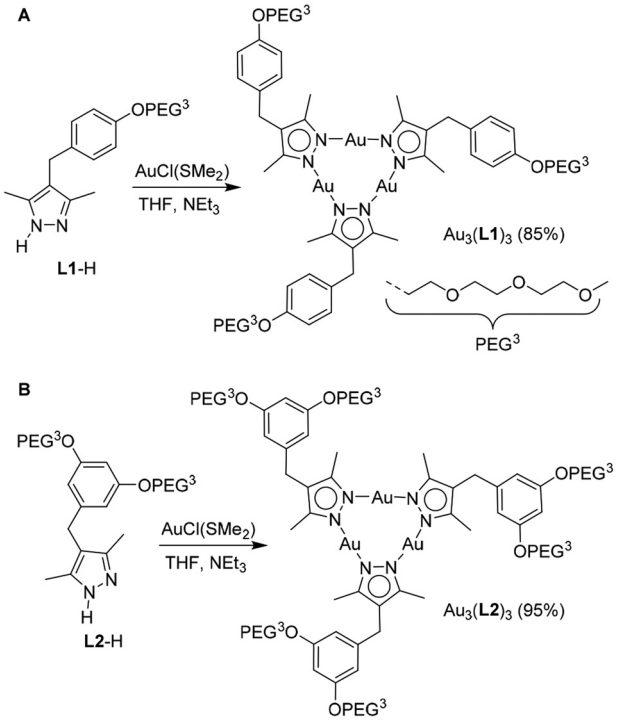

Scheme 1 Synthesis of the amphiphilic gold complexes $\mathbf{Au_3(L1)_3}$ (A) and $\mathbf{Au_3(L2)_3}$ (B).

Results and discussion

In continuation of our efforts to generate nanostructures based on Au_3(pyrazolate)$_3$ complexes,[17,18] we have prepared trinuclear Au(I) complexes with PEG side chains. For this purpose, we have synthesized the pyrazolate ligands **L1**-H and **L2**-H (Scheme 1) by reaction of the respective PEGylated diketones with hydrazine (for details, see the ESI‡). The ligands were then combined with Au(SMe$_2$)Cl in THF in the presence of NEt$_3$ to give the trimeric complexes $\mathbf{Au_3(L1)_3}$ and $\mathbf{Au_3(L2)_3}$ in excellent yields.

With the complexes $\mathbf{Au_3(L1)_3}$ and $\mathbf{Au_3(L2)_3}$ in hand, we proceeded to study the aggregation of the metalloamphiphiles in water. In a typical procedure, a stock solution of Au_3L_3 in MeCN was added under vigorous stirring to water, followed by the removal of the organic solvent under reduced pressure (for more details, see ESI‡). Dynamic light scattering (DLS) analyses of freshly prepared samples revealed the formation of polydisperse aggregates with a wide size distribution. After filtration (pore size: 1.2 μm), we were able to determine an average size of about 330 nm for $\mathbf{Au_3(L1)_3}$ and 400 nm for $\mathbf{Au_3(L2)_3}$ (see the ESI, Fig. S28 and S31‡).

TEM analyses of dried samples showed undefined shapes in the case of $\mathbf{Au_3(L2)_3}$, but spherical particles in the case of $\mathbf{Au_3(L1)_3}$ (see the ESI, Fig. S34 and S35‡). Samples of $\mathbf{Au_3(L1)_3}$ were subsequently examined by cryoEM. The images revealed the presence of multilayer vesicles with an onion-like architecture (Fig. 2A–C). The sizes of the nano onions varied between ~150 and 350 nm, and their spherical shape was corroborated

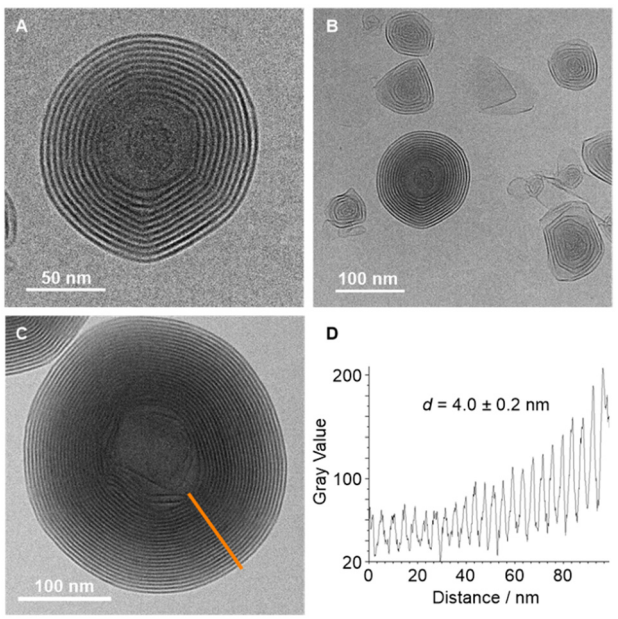

Fig. 2 CryoEM images of the aggregates obtained from $\mathbf{Au_3(L1)_3}$ (A, B and C), the inter-layer distance *d* as determined by gray-scale variations (D).

by cryoEM tomography (see the ESI,‡ CryoEM_Tomography.avi). According to a gray-scale analysis of the images, the distance between the high-contrast parts of the sheets is 4.0 ± 0.2 nm (Fig. 2D). The presence of Au in the nano onions was substantiated by SEM-EDX mapping (see the ESI, Fig. S37‡).

Alongside the spherical aggregates, we were able to detect sheet-like structures (Fig. 2B). The latter are likely precursors for the multilayer vesicles.

CryoEM images of freshly prepared samples showed a larger proportion of sheets and nano onions at incipient stages (see the ESI, Fig. S36‡). Time-dependent zeta potential measurements showed an increase of the potential from −25.3 ± 0.8 mV to around −15 mV in the first five hours, followed by small changes within the next 24 hours (see the ESI, Fig. S28‡). We assume that the increase of the zeta potential is linked to the transformation of sheet structures into nano onions.

In order to examine if the presence of Au(I) was essential for the aggregation process, we synthesized the analogous copper and silver complexes $\mathbf{Cu_3(L1)_3}$ and $\mathbf{Ag_3(L1)_3}$ (Scheme 2). The syntheses proceeded smoothly, and the formation of the complexes was confirmed by NMR spectroscopy and HRMS.

DLS analyses of aqueous solutions containing $\mathbf{Cu_3(L1)_3}$ or $\mathbf{Ag_3(L1)_3}$ revealed the presence of aggregates with an average size of around 200 nm and 158 nm for $\mathbf{Cu_3(L1)_3}$ and $Ag_3(\mathbf{L1})_3$, respectively (see the ESI, Fig. S31 and 32‡). CryoEM images of $\mathbf{Cu_3(L1)_3}$ samples displayed spherical aggregates with a multilayered architecture. However, the orientation of the layers was less ordered when compared to what was observed for $\mathbf{Au_3(L1)_3}$, and one could distinguish multiple domains of parallel sheets within one aggregate (Fig. 3A and B). In the case of the Ag(I) complex $\mathbf{Ag_3(L1)_3}$, the structures of the aggregates were even less defined. Sheets could be identified, but only few of them were arranged in a parallel fashion (Fig. 3C and D). The results imply that the self-assembly process is influenced by the metal ion, with the presence of Au(I) being crucial for the formation of well-defined nano onions.

Attempts to analyze $\mathbf{Au_3(L1)_3}$ by single crystal X-ray diffraction (XRD) were unfortunately not successful. While we were able to obtain single crystals of the complex, the quality of the diffraction data was poor. We suspected that the flexible polyethylene glycol side chains in $\mathbf{Au_3(L1)_3}$ were hampering a structural analysis. Therefore, we synthesized the known complex $\mathbf{Au_3(L3)_3}$[8] with simple benzyl side chains in position 4 of the bridging pyrazolate ligands (Scheme 3).

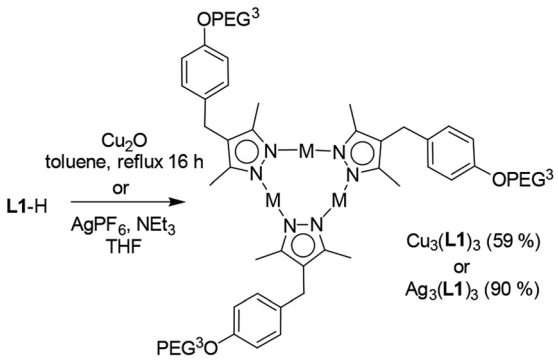

Scheme 2 Synthesis of the complexes $\mathbf{Cu_3(L1)_3}$ and $\mathbf{Ag_3(L1)_3}$.

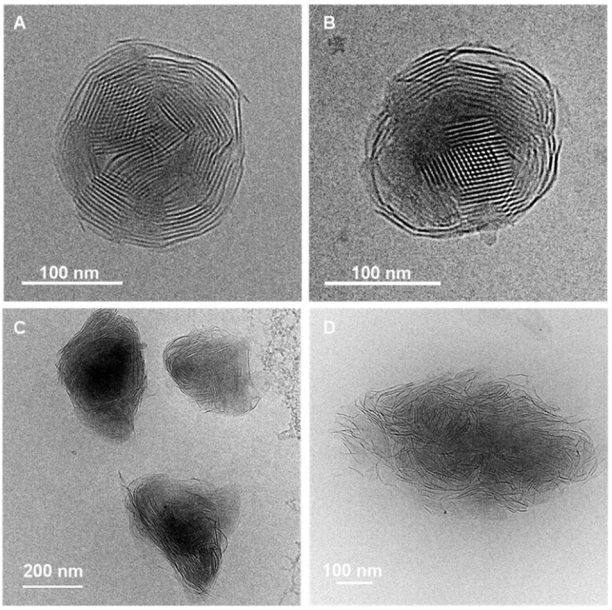

Fig. 3 CryoEM images of the aggregates obtained from $\mathbf{Cu_3(L1)_3}$ (A and B) or from $\mathbf{Ag_3(L1)_3}$ (C and D).

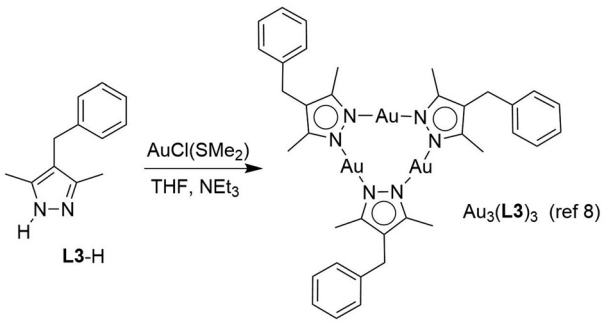

Scheme 3 Synthesis of the complex $\mathbf{Au_3(L3)_3}$.

Single crystals of $\mathbf{Au_3(L3)_3}$ were obtained by slow vapor diffusion of pentane into a $CHCl_3$ solution of the complex and an XRD analysis was performed (Fig. 4). The central Au_3(pyrazolate)$_3$ core of complex $\mathbf{Au_3(L3)_3}$ is planar, and the lengths of the Au–N bonds (1.993–2.007 Å) are within the expected range. The benzyl side chains are not in the same plane as the pyrazolate heterocycles, with two benzyl groups pointing 'up' and one 'down'. The individual Au_3(pyrazolate)$_3$ trimers are arranged in an offset, π-stacked fashion. The coplanar arrangement of the gold trimers gives rise to columns of Au_3(pyrazolate)$_3$ complexes, which are separated by closely packed benzyl groups. The closest intermolecular contact between neighboring Au atoms is 3.6672(4) Å. This value is smaller than the sum of van der Waals radii for Au(I) (3.80 Å),[5b] but longer than the intermolecular Au···Au contacts in previously reported Au_3(pyrazolate)$_3$ complexes (~3.4 Å).[4] It is worth noting that the presence of short Au···Au contacts in Au_3(pyrazolate)$_3$ complexes is often associated with solid-state

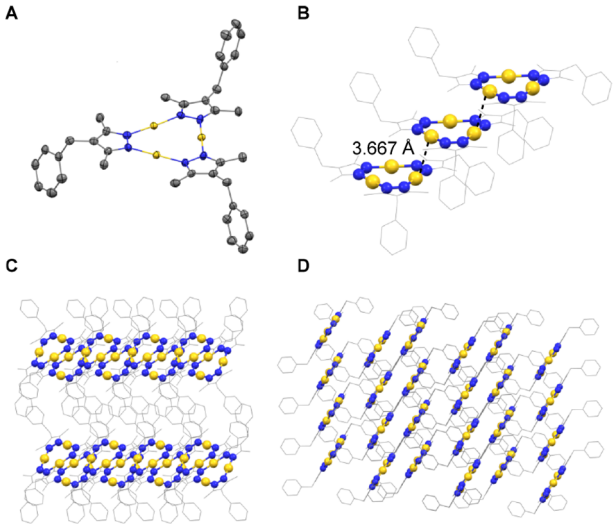

Fig. 4 Molecular structure of $Au_3(L3)_3$ in the crystal with ellipsoids at 50% probability (A). Packing of adjacent $Au_3(L3)_3$ complexes (B). View of the packing inside the crystal (C and D). Color code: Au: yellow, N: blue, C: grey. Hydrogen atoms are omitted for clarity.

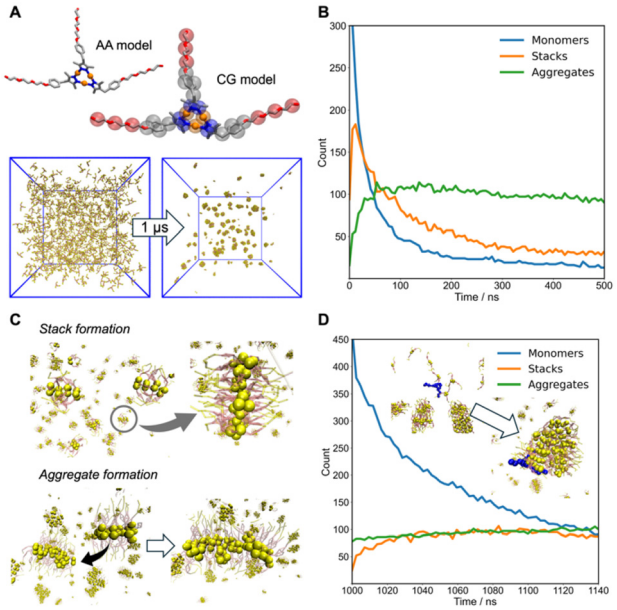

Fig. 5 All-atom (AA) and coarse-grained (CG) models of the $Au_3(L1)_3$ complex used in the simulations (A). Evolution of assemblies over time in a 1 μs (CG time) simulation (B). Stack formation and aggregation (C). Behavior of assemblies after the introduction of 500 additional monomers (D).

luminescence.[4] Solid $Au_3(L3)_3$, as well as the parent complex $Au_3(L1)_3$, were found to be non-emissive.

The structure of $Au_3(L3)_3$ provides hints about possible arrangements of the gold trimers in the nano onions. The high-contrast areas are expected to contain the gold complexes. A gold-rich layer could form by a parallel arrangement of columns made from π-stacked Au_3(pyrazolate)$_3$ complexes. The interface with the water-rich layer would then be provided by the PEG side chains. The nano onions were found to be non-emissive. Therefore, we assume that close Au···Au contacts are not present in the aggregates. The crystal structure of $Au_3(L3)_3$ provides evidence that stacks of Au_3(pyrazolate)$_3$ complexes can form without strong aurophilic interactions. One should note that in aqueous solution, the interaction between the gold trimers is expected to be reinforced by hydrophobic interactions.

To assess the potential of nano onions for the uptake of lipophilic molecules, we conducted uptake experiments using Nile Red. Nile Red's solvatochromic properties allow for easy monitoring of encapsulation in the nano onions. In water, the poorly soluble dye exhibited weak emission with a maximum at 660 nm (see ESI, Fig. S38‡). Once encapsulated within the nano onions, the emission maximum shifted to 636 nm and its intensity significantly increased, indicating successful encapsulation.

To complement the experimental observations, MD simulations were employed to investigate the self-assembly of $Au_3(L1)_3$ complexes at the molecular level (for details, see the ESI,‡ section 9).[19] A coarse-grained (CG) model was developed based on an all-atom (AA) representation of the $Au_3(L1)_3$ complex to enable simulations over larger time and length scales (Fig. 5A). Initial simulations were conducted with 1000 monomers randomly dispersed in the simulation box, allowing us to monitor their dynamic assembly over 1 μs (CG time). We classified the $Au_3(L1)_3$ complexes into three categories based on the spatial arrangement and orientation of their cores: monomers (isolated molecules), stacks (clusters of monomers whose Au atom planes are aligned and in sufficient proximity for stacking interactions), and aggregates (clusters that can contain multiple stacks or non-stacked monomers). This classification allowed us to track the dynamic behaviour of these assemblies over time (Fig. 5B), capturing the rapid decrease in the number of monomers, which assemble into stacks (Fig. 5C) within the first 50 ns (CG time). Beyond this point, the number of stacks gradually decreases over time, as these assemble into larger aggregates, primarily through lateral interactions between the aliphatic chains (Fig. 5C). This observation aligns closely with the XRD analysis of $Au_3(L3)_3$, which revealed columns of offset π-stacked trimers in the solid state. Simulations confirm that similar stacking occurs in aqueous solution, where stacks of 2–4 monomers form. The stacks in solution remain self-limited in size and further assemble into larger aggregates through lateral interactions rather than forming extended fibers. This suggests that the flexible PEG chains in $Au_3(L1)_3$ play a key role in limiting the stack size and promoting lateral growth into larger aggregates, as observed in the nano onion structures. After 1 μs of simulation, an additional 500 monomers were introduced to the system. Fig. 5D shows a continued, rapid decline in the monomer count, while the number of stacks and aggregates remains relatively stable. The stability in the number of stacks implies that their formation becomes limited once larger aggregates are present, and the primary mode of monomer

incorporation shifts toward expanding the aggregates through lateral interactions between the aliphatic chains, contributing to their growth in size rather than in number. This lateral growth mechanism indicates that, over extended time scales, the aggregates can develop into sheet-like structures, consistent with the experimental cryoEM observation of layered nano onions.

Conclusions

We have synthesized an Au_3(pyrazolate)$_3$ complex with three PEG side chains. In aqueous solution, this complex was found to form multilayer vesicles with an onion-like architecture. Thus far, there are only limited reports about the formation of nano onions from metalloamphiphiles.[13–15] To the best of our knowledge, the use of Au(I) complexes is unprecedented in this context.

Control experiments with analogous Ag(I) and Cu(I) complexes highlighted the crucial role of Au(I) in the formation of well-defined nano onions. A structurally related Au(I) complex, lacking solubilizing PEG chains, was examined by single-crystal XRD. In the solid state, columns of offset, π-stacked Au_3(pyrazolate)$_3$ complexes were observed. A similar stacking of gold-trimers could provide the molecular basis for the formation of nano onions. To support this hypothesis, MD simulations were conducted. The simulations revealed that **Au_3(L1)$_3$** complexes first assemble into small stacks, which then aggregate *via* lateral interactions between the side chains, suggesting a lateral growth mechanism in the formation of the larger multilayer vesicles.

Overall, our results provide further evidence for the potential of Au_3(pyrazolate)$_3$ complexes as building blocks in molecular nanoscience.

Author contributions

A.B.S. and K.S. initiated the study, A.B.S. and D.D. performed the experiments and analyzed the data, L.L., M.D.P. and G.M.P. performed the modeling work, F.F.-T. collected and processed the X-ray data, and A.B.S. and K.S. co-wrote the manuscript. All authors discussed the results and commented on the manuscript.

Data availability

Synthetic procedures, experimental and simulation details. Computational materials and data pertaining to the study conducted herein (input files, trajectories, *etc*.) are available at: **https://zenodo.org/records/13828920**.

Conflicts of interest

There are no conflicts to declare.

Acknowledgements

The work was supported by the école Polytechnique Fédérale de Lausanne (EPFL). We thank David Fernando Reyes Vasquez for the EDX measurements and helpful discussions, the mass spectrometry service at EPFL for the HRMS measurements and the materials characterization center at the EPFL. G.M.P. acknowledges the funding received by the European Research Council under the European Union's Horizon 2020 research and innovation program (grant agreement no. 818776-DYNAPOL).

References

1 For selected review articles, see: (*a*) G. Picci, C. Caltagirone, A. Garau, V. Lippolis, J. Milia and J. W. Steed, *Coord. Chem. Rev.*, 2023, **492**, 215225; (*b*) P. Garg, B. Kaur, G. Kaur and G. R. Chaudhary, *Adv. Colloid Interface Sci.*, 2022, **302**, 102621; (*c*) C. Cuerva, M. Cano and C. Lodeiro, *Chem. Rev.*, 2021, **121**, 12966–13010; (*d*) Y. Zhu, W. Zheng and H.-B. Yang, *Chem. Soc. Rev.*, 2021, **50**, 7395–7417; (*e*) P. Sutar and T. K. Maji, *Dalton Trans.*, 2020, **49**, 7658–7672; (*f*) H. Wu, J. Zheng, A.-L. Kjøniksen, W. Wang, Y. Zhang and J. Ma, *Adv. Mater.*, 2019, **31**, 1806204; (*g*) K. C. Bentz and S. M. Cohen, *Angew. Chem., Int. Ed.*, 2018, **57**, 14992–15001; (*h*) Y. Wang, D. Astruc and A. S. Abd-El-Aziz, *Chem. Soc. Rev.*, 2019, **48**, 558–636; (*i*) A. Winter and U. S. Schubert, *Chem. Soc. Rev.*, 2016, **45**, 5311–5357; (*j*) P. Dastidar, S. Ganguly and K. Sarkar, *Chem. – Asian J.*, 2016, **11**, 2484–2498; (*k*) J. Zhang and C.-Y. Su, *Coord. Chem. Rev.*, 2013, **257**, 1373–1408; (*l*) G. R. Whittell, M. D. Hager, U. S. Schubert and I. Manners, *Nat. Mater.*, 2011, **10**, 176–188; (*m*) F. Mancin, P. Scrimin, P. Tecilla and U. Tonellato, *Coord. Chem. Rev.*, 2009, **253**, 2150–2165; (*n*) J. L. Serrano and T. Sierra, *Coord. Chem. Rev.*, 2003, **242**, 73–85.

2 F. Bonati, G. Minghetti and G. Banditelli, *J. Chem. Soc., Chem. Commun.*, 1974, 88–89.

3 G. Minghetti, G. Banditelli and F. Bonati, *Inorg. Chem.*, 1979, **18**, 658–663.

4 For review articles, see: (*a*) J. Zheng, Z. Lu, K. Wu, G.-H. Ning and D. Li, *Chem. Rev.*, 2020, **120**, 9675–9742; (*b*) R. Galassi, M. A. Rawashdeh-Omary, H. V. R. Dias and M. A. Omary, *Comments Inorg. Chem.*, 2019, **39**, 287–348; (*c*) J. Zheng, H. Yang, M. Xie and D. Li, *Chem. Commun.*, 2019, **55**, 7134–7146; (*d*) M. A. Omray, A. A. Mohamed, M. A. Rawashdeh-Omary and J. P. Fackler Jr, *Coord. Chem. Rev.*, 2005, **249**, 1372–1381; (*e*) A. Burini, A. A. Mohamed and J. P. Fackler, *Comments Inorg. Chem.*, 2003, **24**, 253–280.

5 (*a*) N. Mirzadeh, S. H. Privér, A. J. Blake, H. Schmidbaur and S. K. Bhargava, *Chem. Rev.*, 2020, **120**, 7511–7591; (*b*) H. Schmidbaur and A. Schier, *Chem. Soc. Rev.*, 2012, **41**, 370–412; (*c*) H. Schmidbaur and A. Schier, *Chem. Soc. Rev.*, 2008, **37**, 1931–1951.

6 (*a*) E. Beltrán, J. Barberá, J. L. Serrano, A. Elduque and R. Giménez, *Eur. J. Inorg. Chem.*, 2014, 1165–1173; (*b*) H. O. Lintang, K. Kinbara, K. Tanaka, T. Yamashita and T. Aida, *Angew. Chem., Int. Ed.*, 2010, **49**, 4241–4245; (*c*) M. C. Torralba, P. Ovejero, M. J. Mayoral, M. Cano, J. A. Campo, J. V. Heras, E. Pinilla and M. R. Torres, *Helv. Chim. Acta*, 2004, **87**, 250–263; (*d*) S. J. Kim, S. H. Kang, K.-M. Park, H. Kim, W.-C. Zin, M.-G. Choi and K. Kim, *Chem. Mater.*, 1998, **10**, 1889–1893; (*e*) J. Barberá, A. Elduque, R. Giménez, F. J. Lahoz, J. A. López, L. A. Oro and J. L. Serrano, *Inorg. Chem.*, 1998, **37**, 2960–2967; (*f*) J. Barberá, A. Elduque, R. Gimenez, L. A. Oro and J. L. Serrano, *Angew. Chem., Int. Ed. Engl.*, 1996, **35**, 2832–2835.

7 A. Kishimura, T. Yamashita and T. Aida, *J. Am. Chem. Soc.*, 2005, **127**, 179–183.

8 M. Enomoto, A. Kishimura and T. Aida, *J. Am. Chem. Soc.*, 2001, **123**, 5608–5609.

9 For a reviews, see: S. E. Sherman, Q. Xiao and V. Percec, *Chem. Rev.*, 2017, **117**, 6538–6631.

10 For examples, see: (*a*) D. Zhang, Q. Xiao, M. Rahimzadeh, M. Liu, C. Rodriguez-Emmenegger, Y. Miyazaki, W. Shinoda and V. Percec, *J. Am. Chem. Soc.*, 2023, **145**, 4311–4323; (*b*) M. Rosati, A. Acocella, A. Pizzi, G. Turtù, G. Neri, N. Demitri, Nonappa, G. Raffaini, B. Donnio, F. Zerbetto, F. B. Bombelli, G. Cavallo and P. Metrangolo, *Macromolecules*, 2022, **55**, 2486–2496; (*c*) Q. Xiao, J. D. Rubien, Z. Wang, E. H. Reed, D. A. Hammer, D. Sahoo, P. A. Heiney, S. S. Yadavalli, M. Goulian, S. E. Wilner, T. Baumgart, S. A. Vinogradov, M. L. Klein and V. Percec, *J. Am. Chem. Soc.*, 2016, **138**, 12655–12663; (*d*) Q. Xiao, S. Zhang, Z. Wang, S. E. Sherman, R.-O. Moussodia, M. Peterca, A. Muncan, D. R. Williams, D. A. Hammer, S. Vértesy, S. André, H.-J. Gabius, M. L. Klein and V. Percec, *Proc. Natl. Acad. Sci. U. S. A.*, 2016, **113**, 1162–1167; S. Zhang, H.-J. Suna, A. D. Hughes, R.-O. Moussodia, A. Bertin, Y. Chen, D. J. Pochan, P. A. Heiney, M. L. Klein and V. Percec, *Proc. Natl. Acad. Sci. U. S. A.*, 2014, **111**, 9058–9063.

11 For examples, see: (*a*) C. Li, J. Yan, X. Hu, T. Liu, C. Sun, S. Xiao, J. Yuan, P. Chen and S. Zhou, *Chem. Commun.*, 2013, **49**, 1100–1102; (*b*) L. Li, M. Rosenthal, H. Zhang, J. J. Hernandez, M. Drechsler, K. H. Phan, S. Rütten, X. Zhu, D. A. Ivanov and M. Möller, *Angew. Chem., Int. Ed.*, 2012, **51**, 11616–11619; (*c*) R. Dong, Z. Zhong and J. Hao, *Soft Matter*, 2012, **8**, 7812–7821; (*d*) A. Song, S. Dong, X. Jia, J. Hao, W. Liu and T. Liu, *Angew. Chem., Int. Ed.*, 2005, **44**, 4018–4021; (*e*) C. Burger, J. Hao, Q. Ying, H. Isobe, M. Sawamura, E. Nakamura and B. Chu, *J. Colloid Interface Sci.*, 2004, **275**, 632–641.

12 For examples, see: (*a*) L. Guo, D. Xia, Y. Wang, S. Ding, J. Xu, Y. Zhu and B. Du, *Polym. Chem.*, 2024, **15**, 30–39; (*b*) M. Xu, K. H. Ku, Y. J. Lee, J. J. Shin, E. J. Kim, S. G. Jang, H. Yun and B. J. Kim, *Chem. Mater.*, 2020, **32**, 7036–7043; (*c*) J. M. Shin, Y. Kim, H. Yun, G.-R. Yi and B. J. Kim, *ACS Nano*, 2017, **11**, 21332142; (*d*) M.-K. Park, S. Jun, I. Kim, S.-M. Jin, J.-G. Kim, T. J. Shin and E. Lee, *Adv. Funct. Mater.*, 2015, **25**, 4570–4579; (*e*) H. Fan and Z. Jin, *Soft Matter*, 2014, **10**, 2848–2855; (*f*) T. Higuchi, M. Shimomura and H. Yabu, *Macromolecules*, 2013, **46**, 4064–4068; (*g*) H. Yabu, T. Higuchi and M. Shimomura, *Adv. Mater.*, 2005, **17**, 2062–2065.

13 For a review about metal-based vesicles, see: P. Garg, B. Kaur, G. Kaur and G. R. Chaudhary, *Adv. Colloid Interface Sci.*, 2022, **302**, 102621.

14 (*a*) W. L. Odette and J. Mauzeroll, *Langmuir*, 2022, **38**, 4396–4406; (*b*) A. S. Knight, J. Larsson, J. M. Ren, R. B. Zerdan, S. Seguin, R. Vrahas, J. Liu, G. Ren and C. J. Hawker, *J. Am. Chem. Soc.*, 2018, **140**, 1409–1414; (*c*) Y. Wu, H. Tan, Y. Yang, Y. Li, J. Xu, L. Zhang and J. Zhu, *Langmuir*, 2018, **34**, 11495–11502; (*d*) Y. Zhou, J. Chen, J.-T. Li, Z.-B. Lin and S.-G. Sun, *J. Mater. Chem. A*, 2018, **6**, 14091–14102; (*e*) J. Shen, Z. Wang, D. Sun, G. Liu, S. Yuan, M. Kurmoo and X. Xin, *Nanoscale*, 2017, **9**, 19191–19200.

15 (*a*) Z. Wang, X. Li, F. Feng, C. Hong, Z. Sun, W. Tian, K. Yu and H. Liu, *Giant*, 2023, **13**, 100142; (*b*) Y. Zhou, J. Luo, T. Liu, T. Wen, K. Williams-Pavlantos, C. Wesdemiotis, S. Z. D. Cheng and T. Liu, *Macromol. Rapid Commun.*, 2023, **44**, 2200216; (*c*) D.-Y. Wang, L.-J. Ren, H.-K. Liu and W. Wang, *Soft Matter*, 2022, **18**, 8656–8662; (*d*) J. Luo, T. Liu, K. Qian, B. Wei, Y. Hu, M. Gao, X. Sun, Z. Lin, J. Chen, M. K. Bera, Y. Chen, R. Zhang, J. Mao, C. Wesdemiotis, M. Tsige, S. Z. D. Chen and T. Liu, *ACS Nano*, 2020, **14**, 1811–1822; (*e*) H.-Y. Wang, L.-J. Ren, X.-G. Wang, J.-B. Ming and W. Wang, *Langmuir*, 2019, **35**, 6727–6734; (*f*) S. Zhou, Y. Feng, M. Chen, Q. Li, B. Liu, J. Cao, X. Sun, H. Li and J. Hao, *Chem. Commun.*, 2016, **52**, 12171–12174; (*g*) H. Liu, J. Luo, W. Shan, D. Guo, J. Wang, C.-H. Hsu, M. Huang, W. Zhang, B. Lotz, W.-B. Zhang, T. Liu, K. Yue and S. Z. D. Cheng, *ACS Nano*, 2016, **10**, 6585–6596; (*h*) H. Li, H. Sun, W. Qi, M. Xu and L. Wu, *Angew. Chem., Int. Ed.*, 2007, **46**, 1300–1303.

16 (*a*) J. Wang, J. Li, Y. Wang, Z. Li and J. Zhang, *Macromolecules*, 2021, **54**, 7448–7459; (*b*) T. Hao, H. Tan, S. Li, Y. Wang, Z. Zhou, C. Yu, Y. Zhou and D. Yan, *J. Polym. Sci.*, 2020, **58**, 704–715; (*c*) F.-F. Hu, Y.-W. Sun, Y.-L. Zhu, Y.-N. Huang, Z.-W. Li and Z.-Y. Sun, *Nanoscale*, 2019, **11**, 17350–17356; (*d*) N. Arai, K. Yasuoka and X. C. Zeng, *ACS Nano*, 2016, **10**, 8026–8037.

17 N. Eren, F. Fadaei-Tirani and K. Severin, *Inorg. Chem. Front.*, 2024, **11**, 3263–3269.

18 N. Eren, F. Fadaei-Tirani, R. Scopelliti and K. Severin, *Chem. Sci.*, 2024, **15**, 3539–3544.

19 D. Bochicchio and G. M. Pavan, *ACS Nano*, 2017, **11**, 1000–1011.